The Influence of Friction Stir Welded Process Parameters of AA2519-T62 on Joint Quality Defined by Non-destructive Laser Amplified Ultrasonic Method and by Microstructure Analysis

Alexander KRAVCOV[1], Janusz KLUCZYŃSKI[2], Robert KOSTUREK[2], Ondřej FRANEK[1], Nikolaj MOROZOV[1], Lucjan ŚNIEŻEK[2], Pavel SVOBODA[1], Petr KUBEČEK[1]

[1]Czech Technical University in Prague, Faculty of Civil Engineering, Thákurova 7/2077, Prague 6 - Dejvice, 166 29, Czech Republic,
[2]Military University of Technology, Faculty of Mechanical Engineering, Institute of Robots & Machine Design, gen. S. Kaliskiego Street 2, Warsaw, 00-908, Poland

E-mails: [1]kravtale@fsv.cvut.cz; [2]janusz.kluczynski@wat.edu.pl

Abstract

The paper contains the results of a non-destructive laser ultrasound internal structure analysis made on specially prepared friction stir welded joints made of aluminum samples. The process was conducted using four different groups of welding parameters. Different tool rotation speeds and tool traverse speeds were used. The main purpose of the research was to analyze the joint quality using a non-destructive laser amplified ultrasound method. A microstructure analysis was also conducted to compare the results of both tests.

KEY WORDS: *Friction Stir Welding, aluminum alloys, microstructure analysis, laser ultrasonic structuroscopy, non-destructive testing*

1. Introduction

FSW (eng. Friction Stir Welding) is a very promising method in terms of joining aluminum alloys, which are difficult to weld using conventional methods [1-4]. This method is a solid-state welding process, where the joint is formed by plasticizing and mixing two workpieces during the action of a specially design tool on the material to be welded [1, 5-7]. An example of aluminum alloy difficult to weld by conventional means is AA2519 – armor grade alloy used for light military constructions [8, 9]. Due to the relatively high concentration of copper (above 5.3%), solidification of this alloy in traditional welding causes a problem of low melting phase Al2Cu (548oC) and as a result, a high risk of hot cracking [10-12]. Although the low temperature of the FSW process (400-500oC) allows this problem to be avoided, it is still important to properly select welding parameters determining the quality of the obtained joint [13-16].

It is very important to determine the joint quality not only using destructive but also non-destructive methods to analyze joints right after the process. In connection with the growth in usability of FSW technology it is very important to determine the proper joint quality check method to ensure the required welded material properties. Ultrasound testing methods are useful in determining the internal quality of the material including internal and surface inclusions and defects [17-19]. This method is also useful for analyzing material properties by measuring the shear wave velocities [20, 21]. The ability to use a laser to amplify the signal ensures the possibility of analyzing elements whose thickness is greater than 10 millimeters [22].

2. Experimental Background

The workpiece to be joined was a 5 mm thick AA2519-T62 extrusion with the chemical composition presented in Table 1.

Table 1.

Chemical composition of AA2519-T62 extrusion

FFe	SSi	CCu	ZZn	TTi	MMn	MMg	NNi	ZZr	SSc	VV	AAl
00.11	00.08	66.32	00.05	00.08	00.17	00.33	00.02	00.19	00.16	00.10	BBase

[1] Corresponding author.
E-mail address: kravtale@fsv.cvut.cz.

The friction stir welding process was performed a using ESAB FSW Legio 4UT machine with an axial force equal to 17 kN and the tilt angle of the MX Triflute tool set to 2o. The used welding parameters together with a designation of the samples are presented in Table 2.

Table 2.

Welding parameters and designation of samples

Sample designation	Tool rotation speed [rpm]	Tool traverse speed [mm/min]
T41	400	100
T81	800	100
T82	800	200
T84	800	400

The joint was determined along the entire length of the weld and also perpendicularly to the traverse transition direction. This kind of analysis were made using optoacoustic equipment and a measuring technique basing on the generation of an ultrasonic signal with ultrashort, high power pulses amplified by an Nd: YAG laser [23]. Additionally, the samples were sectioned perpendicularly to the welding direction and were metallurgically examined. The microstructure investigation was performed using an Olympus LEXT OLS 4100 digital light microscope. As part of the metallographic sample preparation, samples were mounted in resin, ground with abrasive paper of 80, 320, 600, 1200, and 2400 gradations, and polished using diamond pastes (3 and 1 μm gradation). The samples were etched using Keller reagent (20 mL H2O + 5 mL HNO3 + 2 mL HF + 1 mL HCl) with an etching time equal to 5s.

3. Results and Discussion

The internal structure of the samples was shown in Figure 1. In both samples where the traverse speed was 100 mm/min (T41 & T81) some imperfections can be observed visible as different colored structures and wave shape distortion. This could also be connected with the density change which is caused by the welding process. As can be seen, the wave shape distortions are present in the samples obtained with the lowest tool traverse speed, which entails the longest affecting time of the tool on welded AA2519-T62.

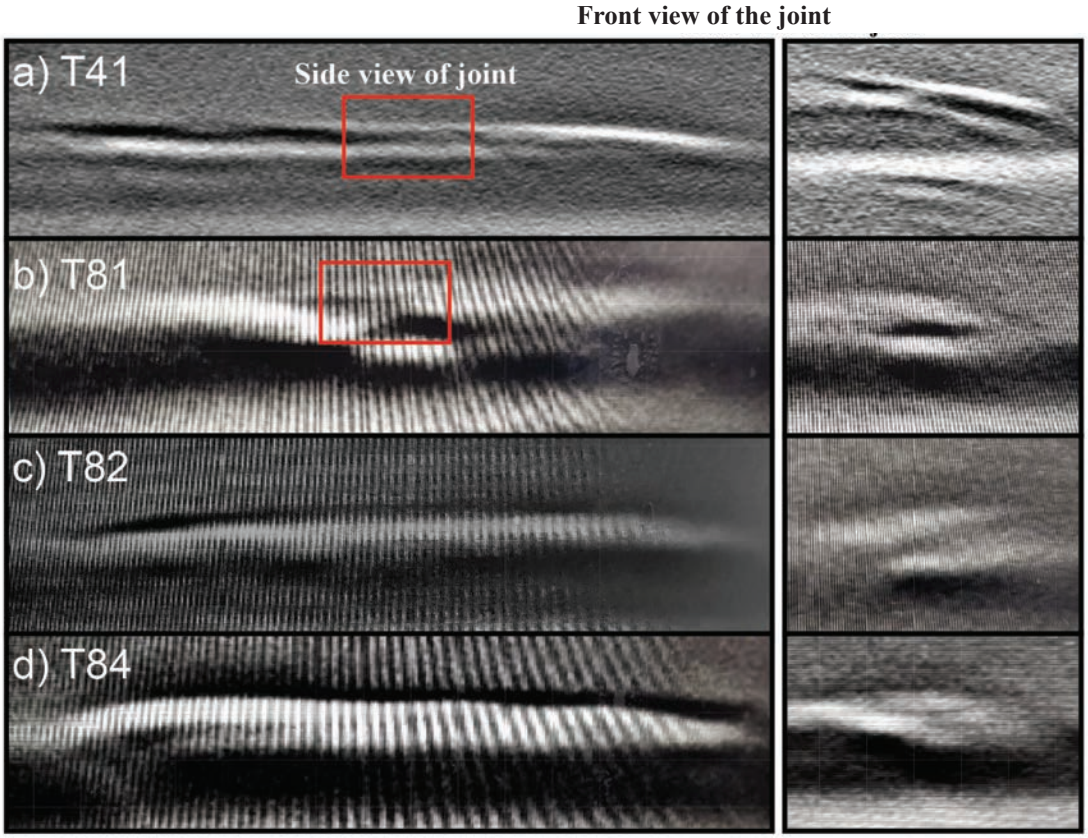

Fig. 1. Internal structure of FSW samples: (a) imperfection in the middle of the T41 joint (red box) – material density change, (b) imperfection in the middle of the T81 joint (red box) – voids and material density change, (c) regular structure of the T82 joint stir zone, (d) regular structure of the T84 joint stir zone.

This leads to phenomena such as substantial dissolution and coarsening of the strengthening phase, as well as fragmentation of the remaining Al2Cu precipitates in the stir zone, and it can partly explain the wave distortions in Fig. 1 [14].

In the course of scanning, local velocities are determined. The velocities dependent on density are related to local modules of elasticity; they can be calculated as follows:

$$E = \rho C_t^2 \left[3 - \frac{1}{x^2 - 1} \right], \tag{1}$$

$$G = \rho C_t^2, \tag{2}$$

where: E is Young's modulus. Note that an S-wave pulse is recorded in the interval between the first and second reflections of P-waves from the back side; the time delay of the S-wave's arrival can be used to calculate its velocity.

Density was determined by hydrostatic weighing of the samples in distilled water. Mean of density AA2519 alloy. The average obtained values of the elastic moduli for the aluminum alloy were *E=67,5GPa* and *G=28,5GPa.*

Distinctly distinguishable zones of recrystallization and thermomechanical affection relative to the base material. During the scan, it was found that the elastic modules in the thermo-mechanically affected zone and the recrystallization zone are reduced by 15%, relative to the base material. The changes in elastic modules in these areas can be explained by far-reaching changes in the welded material microstructure. The mechanical properties of AA2519 are mostly determined by the presence of the strengthening phase and during the FSW process this phase undergoes disadvantageous evolutions mostly in the recrystallization zone and thermo-mechanically affected zone [1,4].

To verify the results from the ultrasound method, light microscope observations were performed. The macrostructure of the T81 joint is presented in Figure 2 with the retreating and advancing side situated on the right and left side, respectively. The macrostructure consists of zones typical for the FSW process: the dynamically recrystallized stir zone (SZ), thermo-mechanically affected zone (TMAZ), heat-affected zone (HAZ) and base material (BM). The microstructure analysis of the T81 sample did not reveal any imperfections in the joint.

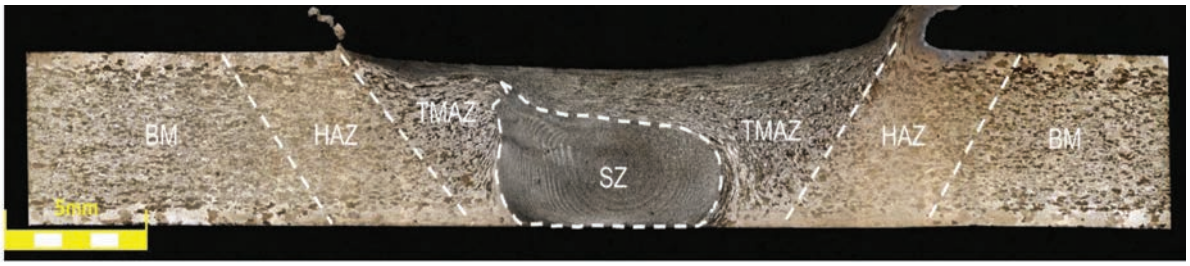

Fig. 2. Macrostructure of T81 joint.

At the same time in samples T41, T82 and T84, the light microscopy observations allowed imperfections to be identified, which are presented in Figure 3.

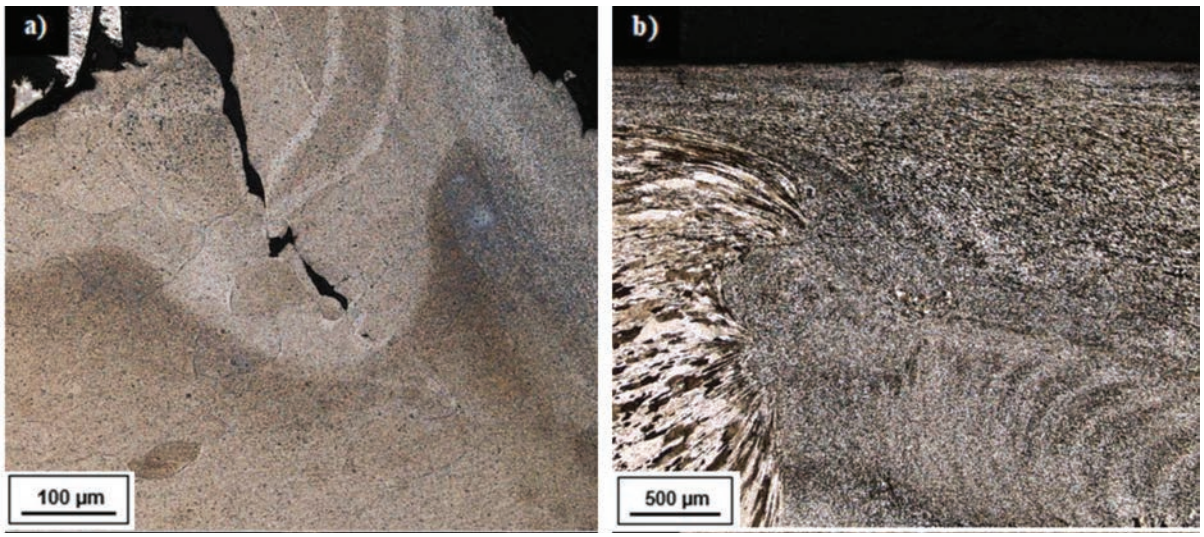

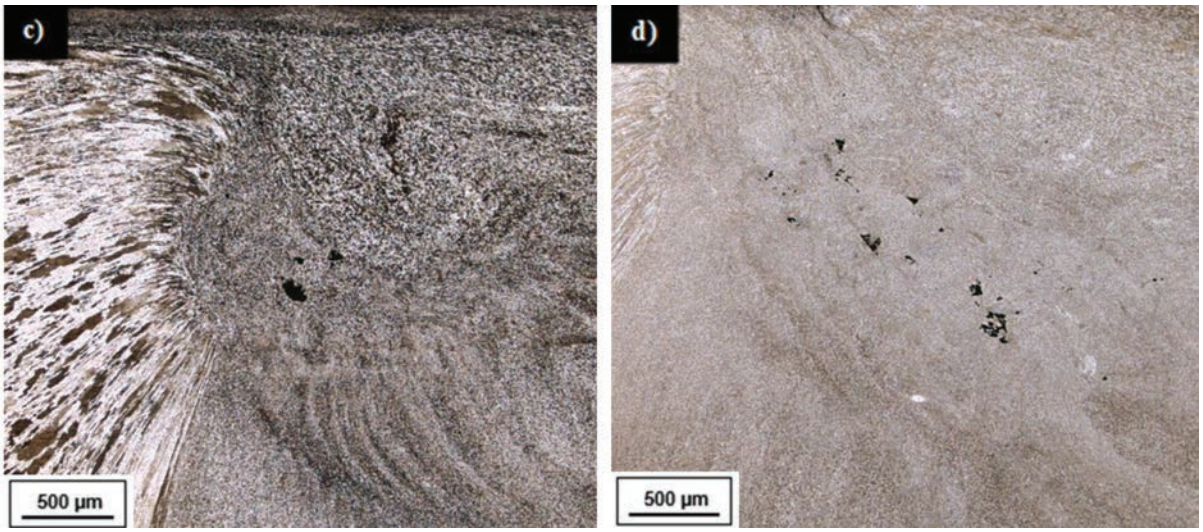

Fig. 3. Microstructure of: (a) imperfection close to the flash in the T41 joint, (b) imperfection-free upper part of the T81 joint stir zone, (c) voids in the upper part of the T82 joint stir zone, (d) voids in the upper part of the T84 joint stir zone.

In the case of the T41 sample, the low value of the tool rotation speed (400 rpm) causes the formation of imperfections close to the flash on the advancing side of the joint as a result of insufficient material plasticization (Fig. 3a). The investigation of the T82 and T84 samples revealed imperfections in the form of voids localized in the upper part of the stir zone (Fig. 3c,d). The number of voids increases together with increasing tool traverse speed value. As can be observed, the same area in the T81 sample is characterized by a lack of visible voids (Fig. 3d). Higher values of tool traverse speed result in decreasing time in which the tool affects the workpiece by friction, and this can cause the presence of imperfections in the joint. It is a noteworthy fact that all imperfections identified by microstructure analysis are localized on the advancing side of the joints, which corresponds to lower heat input than the retreating side. Although insufficient heat input is the main reason for low joint quality, the character of the imperfections differs depending on the welding parameters.

4. Conclusions

As a result of the work, it was possible to diagnose the technology of friction stir welding with the help of laser-ultrasonic structuroscopy and the subject of the presence of continuity defects. A method for determining Young's modulus and shear modulus is presented. The study showed that the decrease in the value of the elastic moduli of the recrystallization region and thermo-mechanically affected zone was on average 15%.

During the analysis of the microstructure, it was determined that high values of tool traverse speed lead to the appearance of defects in the joint. Most of the specific defects are localized on the advancing side of the joint.

Acknowledgement

This research was financially supported by the National Ministry of Education of Czech Republic (No. 027/0008465). In addition, authors would like to acknowledge the financial support from the Polish Ministry of National Defence (No. PBG/13-998). The authors also want to thank Lt.Col. Dr. Ing. Paweł Maciejewski (War Studies Academy) and the Czech Technical University for hosting the authors as visiting scholars from May 2019 to August 2019.

References

1. **Mishra, R.S.; Mahoney, M.W.,** Friction Stir Welding and Processing; ASM International: Materials Park, OH, USA, 2007; ISBN 978-0-87170-840-3.
2. **Rao, C.V., Reddy, G.M., Rao, K.S.,** Microstructure and pitting corrosion resistance of AA2219 Al–Cu alloy friction stir welds — Effect of tool profile. Def. Technol. 2015, 11, 123–131.
3. **Babu, S.; Elangovan, K.; Balasubramanian, V.,** Optimizing friction stir welding parameters to maximize tensile strength of AA2219 aluminium alloy joints. Met. Mater. Int. 2009, 15, 321–330.
4. **Sabari, S.S.; Malarvizhi, S.; Balasubramanian, V.,** Characteristics of FSW and UWFSW joints of AA2519-T87 aluminium alloy: Effect of tool rotation speed. J. Manuf. Process. 2016, 22, 278–289.

5. **Kosturek, R.; Wachowski, M.; Ślęzak, T.; Śnieżek, L.; Mierzyński, J.; Sobczak, U.,** Research on the friction stir welding of Titanium Grade 1. In Proceedings of the International Conference on Advanced Functional Materials and Composites (ICAFMC2018), MATEC Web of Conferences 242, Barcelona, Spain, 5–6 September 2018.
6. **Zhang, Z.; Xiao, B.L.; Ma, Z.Y.,** Effect of welding parameters on microstructure and mechanical properties of friction stir welded 2219Al-T6 joints. J. Mater. Sci. 2012, 47, 4075–4086.
7. **Liang, X.P.; Li, H.Z.; Li, Z.; Hong, T.; Ma, B.; Liu, S.D.; Liu, Y.,** Study on the microstructure in a friction stir welded 2519-T87 Al alloy. Mater. Des. 2012, 35, 603–608.
8. **Fisher, J., James, J.,** Aluminum alloy 2519 in military vehicles. Mater. Sci. Forum 2002, 160, 43–46.
9. **Wu, Y.P., Ye, L.Y., Jia, Y., Liu, L., Zhang, X.M.,** Precipitation kinetics of 2519A aluminum alloy based on aging curves and DSC analysis. Trans. Nonferrous Metal. Soc. China 2014, 24, 3076–3083.
10. **Schaer, G.B., Sercombe, T.B., Lumley, R.N.,** Liquid phase sintering of aluminium alloys. Mater. Chem. Phys. 2001, 67, 85–91.
11. **Stoichev, N.V., Yaneva, S.B., Regel, L.L., Videnskiy, I.V.,** Eutectic solidification of Al–Cu alloys influenced by convection. Adv. Space Res. 1998, 8, 171–174.
12. **Gündüz, M.; Çadirli, E.,** Directional solidification of aluminium–copper alloys. Mater. Sci. Eng. A Struct. 2002, 327, 167–185.
13. **Xu,W.F.; Liu, J.H.; Chen, D.L.; Luan, G.H.,** Low-cycle fatigue of a friction stir welded 2219-T62 aluminium alloy at different welding parameters and cooling conditions. Int. J. Adv. Manuf. Technol. 2014, 74, 209–218.
14. **Kosturek, R.; Śnieżek, L.; Wachowski, M.; Torzewski, J.,** The Influence of Post-Weld Heat Treatment on the Microstructure and Fatigue Properties of Sc-Modified AA2519 Friction Stir-Welded Joint. Materials 2019, 12, 583.
15. **Kosturek, R., Śnieżek, L., Torzewski, J., Wachowski, M.,** Research on the Friction Stir Welding of Sc-Modified AA2519 Extrusion. Metals 2019, 9, 1024.
16. **Kosturek, R., Śnieżek, L., Torzewski, J., Wachowski, M.,** Research on the friction stir welding of Sc-modified AA2519 extrusion, Metals, Volume 9, Issue 10, October 2019, Article number 1024, https://doi.org/10.3390/met9101024
17. **Stoller, J., Zezulova, E.,** Use of ultrasound-The ultrasonic pulse velocity method for the diagnosis of protective structures after the load of TNT explosion, pp. 230-235 in ICMT 2017 - 6th International Conference on Military Technologies. https://doi.org/10.1109/MILTECHS.2017.7988761
18. **Svoboda, P., Kravcov, A., Pospíchal, V., Morozov, N., Zezulová, E.,** Quality assessment of bored pile foundations by a set of non-destructive testing methods, ICMT 2019 - International Conference on Military Technologies 2019. Brno https://doi.org/10.1109/MILTECHS.2019.8870062
19. **Štoller J., Dvorak P.,** Ultrasound Diagnosis of Protective Structures after Contact Explosion. In: Transport Means 2014. Kaunas, Lithuania: Kaunas University of Technology, Lithuania, 2014, p. 264-267. ISSN 2351-4604
20. **Kravcov, A., Shibaev, I.,** Measurement of local mechanical characteristics of marble by broadband ultrasonic structuroscopy, International Journal of Civil Engineering and Technology (IJCIET). 2019, 10 35-42. ISSN 0976-6308
21. **Quintero R., Simonetti F., Sellinger A.,** Noncontact laser ultrasonic inspection of Ceramic Matrix Composites (CMCs), NDT & E International 88, 8-16, 2017
22. **Kravcov, A., Shibaev, I.,** "Examination of structural members of aerial vehicles by laser ultrasonic structuroscopy," International Journal of Civil Engineering and Technology, vol. 9, issue 11, pp. 2258-2265, November 2018.
23. **Kravcov, A., Platek, P., Pospichal, V., Koperski, W.,** Internal structure research of 3D printed cellular structures by laser-ultrasonic structuroscopy, ICMT 2019 – International Conference on Military Technologies 2019. Brno, https://doi.org/10.1109/MILTECHS.2019.8870047